

CHAPTER 3

**Molecular docking and expression studies of
LG extract for Molecular target(s)
identification**

5.0 INTRODUCTION

Osteoporosis, known as the “silent disease”, occurs in women and men, is associated with a loss of bone mass and increased risk of fracture. Osteoporosis prevalence in the world is very high; it affects around 200 million people and has become a major determinant of morbidity, mortality and disability of aged people (Martinis et al., 2019). Due to the disadvantages associated with these therapies, it has been challenging to identify new therapy or molecule for osteoporosis treatment. Therefore, researchers have focused on developing the medicine from herbals which have a unique benefit in the treatment of various diseases, including osteoporosis (Yang F et al., 2019). There are many herbals that have been studied and discovered for their anti-osteoporotic properties like Sulfuretin, Genistein, Diosgenin etc (Cotter et al., 2003; Miao et al., 2012; Suvarna et al., 2018). Further, Plants like *Cissus quadrangularis*, *Withania somnifera*, *Tinospora cordifolia* and *Punica granatum* are studied for its effects and it was established to be found effective in the management of osteoporosis (Shubhashree, 2018). Group of scientist have successfully identified a range of phytocomponents like Salvianolic acid B, Ugonin K, Kireinol which have been proved to anti-osteoporotic properties (Cui et al., 2012; Suvarna et al., 2018). Phytochemical analysis of *S. miltiorrhiza* revealed that it contains multiple groups of compounds, the main constituents of which include phenolics (protocatechuic aldehyde, salvianolic acid A, and salvianolic acid B) and tanshinones (tanshinone I, tanshinone IIA, cryptotanshinone, 15, 16-dihydrotanshinone I). Some phytochemicals have antioxidative activity and/or estrogen-like activity. They produce bone protective effects, through estrogen receptor and/or improving antioxidative capacity, and some may directly regulate the proliferation and activity of osteoblast and osteoclast (Jia et al., 2012). *Epimedium* is the herbal medicinal plants and has been used since long time to combat osteoporosis and menopause-related diseases in China. It is also used throughout the ages as an anti-osteoporotic agent. The phytochemical analysis of the crude extract of *Epimedium* flavonoids has shown that it contains epimedin B, icariin and epimedin C. These compounds have been identified as the key

antiosteoporotic constituent of Epimedium plants by triggering bone formation, inhibiting bone resorption and blocking urinary calcium excretion. It has also been demonstrated to prevent osteoporosis without causing uterine hyperplasia in the ovariectomized rat model (Ma et al., 2011; Tantry et al., 2012; Liu X L et al., 2017; Jolly et al., 2018). Another such herbals is *Litsea glutinosa* (LG) also known as “Maida Lakri”, is known to be one of the most potent plants for treatment of osteoporosis (Sukhdev, 2006) and has been reported with numerous benefits like anti-inflammatory, wound healing activity (Sharma et al., 2019). It has been identified to cure chronic coughs (Rahmatullah et al., 2012), it has also been used for drug development for cardiac diseases (Mehrotra et al., 2007). In *CharakaSamhita*, it is classified as jivaniya and has been reported to retain properties like antibacterial, antioxidant, hypotensive, antipyretic and chemoprotective (Unnikrishnan, 2016). Studies by Parikh and co-workers (Parikh, 2009 & 2012; Rangrez et al., 2011) have also proved osteoprotective properties of LG in OVX rats and have reported reduced serum TRAcP (Tartrate-resistant acid phosphatase) levels, restored ALP (alkaline phosphatase) and reduced rate of Ca^{++} excretion. Further, they have analysed the methanolic extract of LG using UV-VIS-IR spectrometry GC-MS analysis and they have opined that it contains many bioactive compounds, such as alkaloids, phenols, tannins, flavonoids, glycosides and saponins. GC analysis further confirmed the presence of various phytochemicals like Oleic acid, tricosene, Androstane, erucic acid, pyridine, tetra decanoic acid, pyrrolidinone, thiocoumarin, piperidine, eicosanoic acid, Alkaloid fraction Eicosane, Pieprizine, Androsta-trione, pregnene, tetrahydroisoquinoline, crinamine etc. Out of these, some are phytoestrogens like Androstane, Pregene. Plant polyphenols are the compounds of great interest because they possess anti-osteoporosis properties and potential antioxidant activity in their function and work as free radical scavengers (Weaver et al., 2012). Food supplements and bone health-promoting effects of flavonoids, polyphenols, isoflavones, and additional phytochemicals are now well investigated. Phytoestrogens are nonsteroidal polyphenolic secondary plant metabolites (isoflavonoids, flavonoids (flavones, flavanones, chalcones), lignans and stilbenes which acts as a potential

replacement for estrogen deficiency and is useful in prevention and treatment of postmenopausal osteoporosis. An in-depth understanding of the effective phyto-compounds in medicinal plants is the crucial to the research and development of medicinal plants. Therefore, the constituent information of any herbal and the construction of its compound database are highly imperative for their application. The construction of a compound database can effectively manage the large quantities of compounds found in medicinal plants (Yi et al., 2018).

However, till date there is no data available pertaining to the exact mode of action of LG at the molecular targets the results of the phytochemical analysis of LG encouraged us to explore the possible target protein of these phytoestrogens and other phytochemicals. Hence, to delaminate the mode of action, the present study is an attempt made to understand the network pharmacology using an in-silico approach for the identification of probable protein targets, followed by an experimental in-vitro approach via studying gene expression pattern of obtained target protein in osteoblastic Saos-2 cell line.

5.1 MATERIAL & METHODS:

5.1.1 PREPARATION OF LG EXTRACT:

Bark powder of LG was purchased from the local market and 50 g was suspended in 500 mL methanol (SA8SF68037, Merck, USA), incubated overnight at room temperature on a magnetic stirrer (REMI, 1 MLH, India). After incubation, the solution was filtered through Whatman® filter paper (MN615A, MN, Germany) to remove insoluble particles. The methanolic extract was allowed to air dry. Upon drying, remaining solid extract was collected, weighed and stored at -20°C for further experiment.

5.1.2 CULTURING OF SAOS-2 CELLS:

Saos-2 cell line was procured from National Center for Cellular Science Institute (NCCS, Pune, India). Cells were maintained throughout in maccoy's 5A (16600082, Gibco, USA) + 10 % FBS media (RM9955-100ML, Himedia, India) at 37°C in CO₂ humidified chamber. For passaging, cells were washed with 1x PBS, followed by trypsinization (TCL099, Himedia, India). After detachment of cells, trypsin was diluted approx. (minimum 1:10) with media. These cells were counted using hemocytometer and were seeded to the fresh flask at a seeding density of 0.4 M/mL.

5.1.3 LG TREATMENT:

The methanolic extract was weighed 250 mg and it was dissolved in the final volume of 1 mL of DMSO (D8418, Sigma, St. Louis, USA), generating 250 mg/mL stock solution. Cells were seeded a day before treatment in T25 flask and serial dilutions of LG extract were prepared in cell culture media (maccoy's 5A (16600082, Gibco, USA) + 10% FBS (10270106, Gibco, USA)) from stock solution to achieve 250 µg/mL, 100 µg/mL & 50 µg/mL working solutions and was filtered by 0.2 µ filter prior to treatment. Tests flasks, control (untreated cells) and vehicle control flasks were incubated at the same conditions for 96 hrs. LG doses were selected based on previous lab studies.

5.1.4 TRANSCRIPT ANALYSIS:

5.1.4.1 TOTAL RNA ISOLATION AND CDNA SYNTHESIS:

Cells from all the flasks were trypsinized. They were resuspended in TRIzol® reagent (15596026, Invitrogen, USA) for total RNA isolation. TRIzol® reagent manual protocol was followed to isolate and purify total RNA. After purification, RNA concentration was estimated by NanoDrop C at 260 nm. First strand of cDNA was synthesized using Thermo cDNA synthesis kit, 5 µg of total RNA was used. cDNA was converted using oligoDT primers using manual protocol (K1612, Thermo, USA). Once cDNA was synthesized, it was then used neat as a template for transcript analysis of desired genes.

5.1.4.2 QUANTITATIVE PCR:

cDNA was used directly as a sample for real time PCR (Quant Studio, Thermo, USA) to analyze the expression level of target genes. Different sets of primers (Table C3. 2) were used for transcript analysis using PowerUP Sybr® green master mix (A25742, Thermo, USA). A standard manual PCR conditions (Table C3. 1) were used for amplification the experiment was performed in triplicates (n=3).

Protein Sequence details of finalized target proteins were extracted from UniProt online protein data base (<https://www.uniprot.org/>). These sequences were used to design primers for real time PCR. Primers were designed using online primer designing tool (www.eurofinsgenomics.eu) and synthesized outsourced (Sigma, St. Louis, USA).

Table C3. 1: Real time PCR conditions

Stage name	Conditions	Cycles/ramp rate
Initial denaturation	95 °C for 5 min	1 cycle
Amplification stage	95 °C for 15 sec	40 cycles
	60 °C for 30 sec	
	72 °C for 45 sec	
Melt curve generation	95 °C for 15 sec	Ramp rate 1.6°C/sec
	60 °C for 1 min	Ramp rate 1.6°C/sec

	95 °C for 15 sec	Ramp rate 0.15°C/sec
--	------------------	----------------------

Table Indicates PCR conditions used for amplifying target gene.

Table C3. 2: Primer details

	Gene Name	RefSeq ID	T _M value (°C)	Primer Type	Sequence
1	DRD2	NM_000795.4	62	Fw	5' CAATACGCGCTACAGCTCCAAG 3'
			62	Re	5' GGCAATGATGCACTCGTTCTGG 3'
2	SC6A3	NM_001044.5	61	Fw	5' CCTCAACGACACTTTTGGGACC 3'
			62	Re	5' AGTAGAGCAGCACGATGACCAG 3'
3	GCR	NM_000176.3	60	Fw	5' GGAATAGGTGCCAAGGATCTGG 3'
			61	Re	5' GCTTACATCTGGTCTCATGCTGG 3'
4	ANDR	NM_000044.6	61	Fw	5' ATGGTGAGCAGAGTGCCCTATC 3'
			63	Re	5' ATGGTCCCTGGCAGTCTCCAAA 3'
5	CP19A	NM_000103.4	61	Fw	5' GACGCAGGATTTCCACAGAAGAG 3'
			64	Re	5' ATGGTGTGTCAGGAGCTGCGATCA 3'
6	NR1I3	NM_001077482.3	62	Fw	5' GCAGAAGTGCTTAGATGCTGGC 3'
			61	Re	5' GCTCCTTACTCAGTTGCACAGG 3'
7	ACTB	NM_001101.5	66	Fw	5' GCAACGGAACCGCTCATT 3'
			67	Re	5' AGCTGAGAGGGAAATTGTGCG 3'

Table C3. 2 Indicating details of primers of all the genes along with T_m value and Gene RefSeq ID of each gene from NCBI. β-Actin was taken as an endogenous control & vehicle control was taken as test control in real time PCR to calculate ΔΔC_T and thereby RQ ΔΔC_T is calculated from ΔC_T mean using the following formula.

$$\Delta C_T = (\text{Test gene } C_T - \text{Endogenous gene } C_T)$$

$$\Delta\Delta C_T = (\Delta C_T \text{ of test sample} - \Delta C_T \text{ of experiment control})$$

$$\text{Relative quantification} = 2^{-\Delta\Delta C_T}$$

5.1.5 STATISTICAL ANALYSIS

All the data were statically analysed. Dunnett's multiple comparisons test was used for statistical analysis. The statistical analysis was performed using one-way ANOVA using GraphPad Prism 8.3.1 Software to obtain p-value each sample was compared with control. (*- $p < 0.05$; **- $p < 0.01$) All the data are presented as mean \pm S.E. and are representative of three independent experiments (n=3).

5.1.6 DATABASE CONSTRUCTION AND TARGET PREDICTION:

Chemical SMILES structures of ingredients were found from online software PubChem. These formulae were imported in the online SwissTargetPrediction network database (<http://www.swisstargetprediction.ch/>) (Gan et al., 2019) to identify possible target proteins in *Homo sapiens* species. Results were received in the form of binding Probability for Androstane, Cinnamic Acid, Cinnamolaurine, Cinnamon, Crinamine, Gestonorone, Piperzine carobnitrile, Piperzine derivative and Thiocoumarin compounds. SMILES formula of each molecule was used to run target prediction (Table C3. 3).

Table C3. 3: Drug name and SMILES formula

Sr No	Compound Name	SMILES formula
1	Androstane	<chem>C1CC(=O)CC2CCC3C4CCC(=O)C4(C)CC(=O)C3C12C</chem>
2	Cinnamic Acid	<chem>Nc1ccccc1CC(Cc1ccccc1)C(=O)O</chem>
3	Cinnamolaurine	<chem>CN1CCc2cc3OCOc3cc2C1Cc1ccc(O)cc1</chem>
4	Cinnamon	<chem>O=C1Oc2ccc([N+](=O)[O-])cc2CC1c1ccc(O)c(O)c1</chem>
5	Crinamine	<chem>COC1C=CC23C(C1)N(CC2O)Cc1c3cc2OCOc2c1</chem>
6	Gestonorone	<chem>CC(=O)C1(O)CCC2C3CCC4=CC(=O)CCC4C3CCC12C</chem>
7	Piperzine carobnitrile	<chem>NCC1C(O)NC(=O)C(C1C)C=N</chem>
8	Piperzine derivative	<chem>CCCCCN1CCN(C(=O)Cc2ccc([O-])c([O-])c2)CC1</chem>
9	Thiocoumarin	<chem>Cc1ccc2c(c1)CC(=O)CC2(C)C</chem>

5.2 RESULTS:

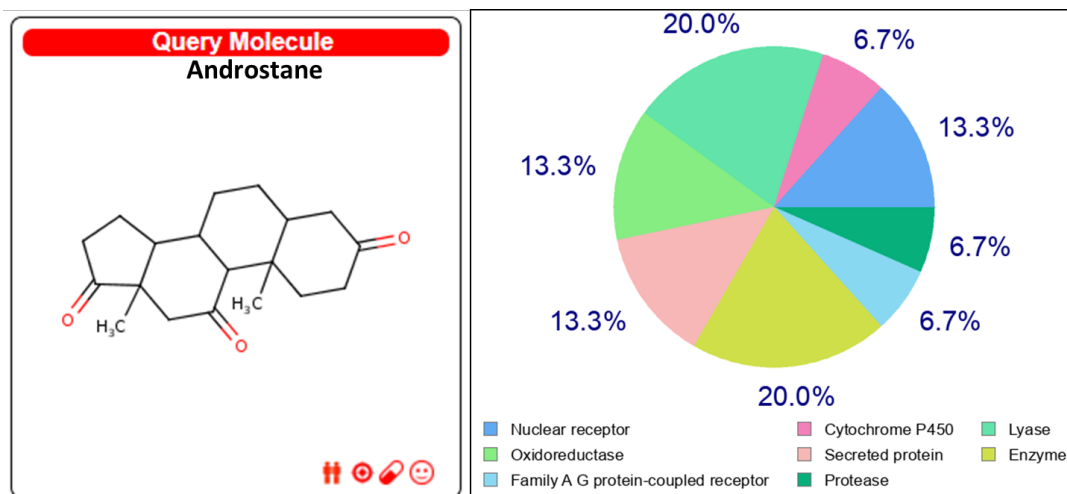
5.2.1 EXTRACTION:

The total yield obtained from LG methanolic extraction was 4.42 gm, which corresponds to ~8.8% total yield.

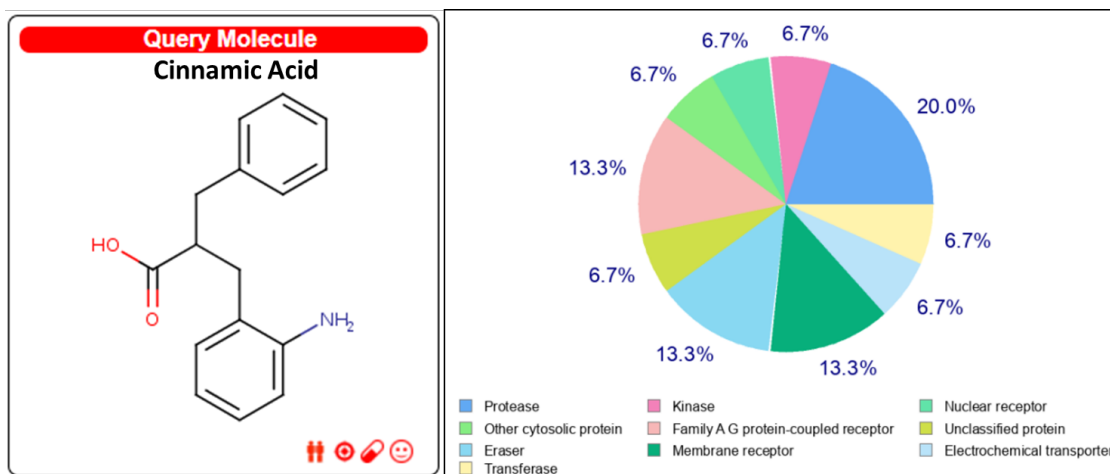
5.2.2 TARGET PREDICTION:

Target prediction using online software Swiss Target Prediction delivered the results for Androstane, Cinnamic Acid, Cinnamolaurine, Crinamine, Gestonorone, Thiocoumarin, Cinnamon, Piperzine carbonitrile and its derivatives. Results were obtained in form of Pie charts, indicating categorisation of target protein, as well as target protein with binding probability.

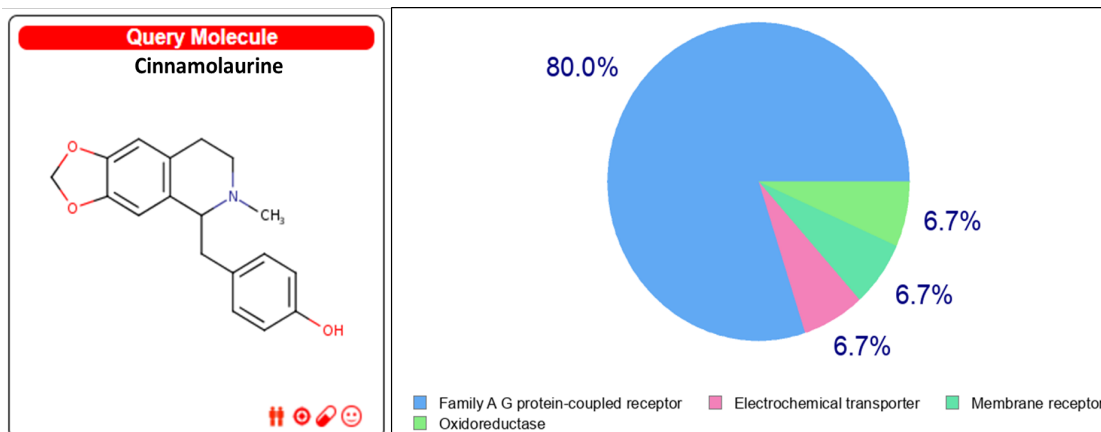
Figure C3. 1 indicate structure of respective phytochemical and its pie charts. Each Pie chart explains % of Protein class of total target proteins belonging to a particular protein class. Some of the molecules like Androstane, cinnamic acid, Gestonorone, crinamine and Thiocoumarin exhibited binding in diversified protein classes including nuclear receptor, cytochromes, enzymes, proteases, Kinases, GPCRs and transporters. Whereas compounds like Cinnamolaurine, Cinnamon and Piperzine carbonitrile and its derivative demonstrated binding with some specific class of protein compared to other classes. Elaborating, Cinnamolaurine and Cinnamon showed 80.0 % and 40.0 % of binding with GPCRs and Kinase class of proteins respectively. Similarly Piperzine carbonitrile and its derivative showed majority of binding with GPCRs in the range of 40.0 % - 66.6 %.



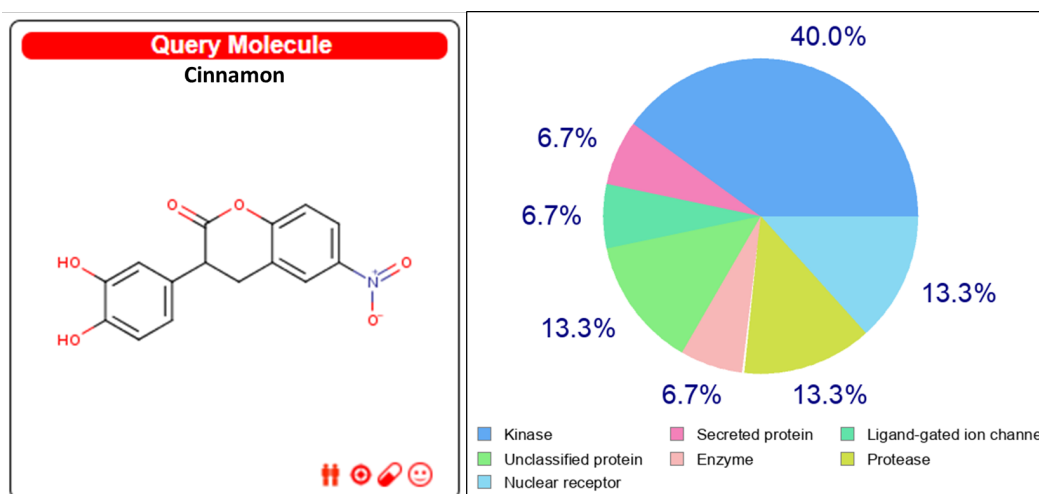
(A) Androstane structure and Pie chart indicating Target proteins class distribution



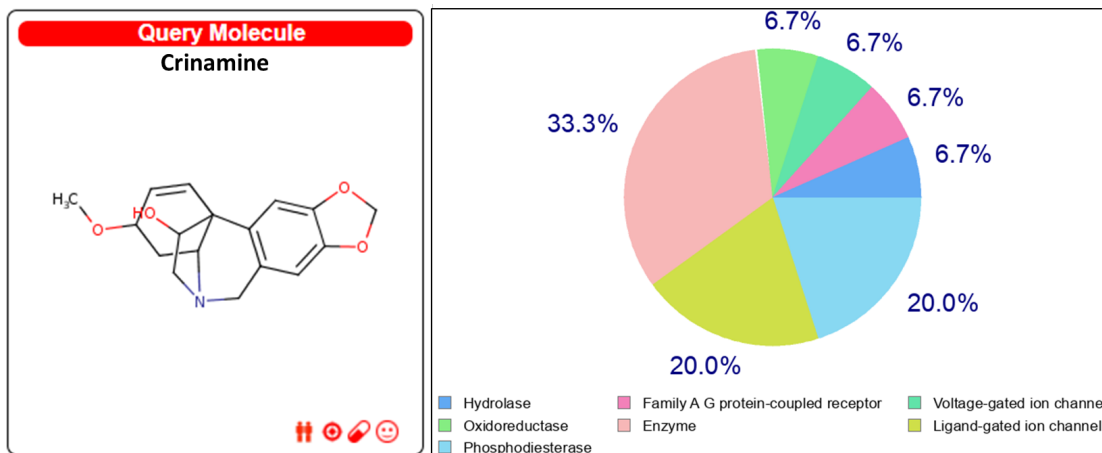
(B) Cinnamic acid structure and Pie chart indicating Target proteins class distribution



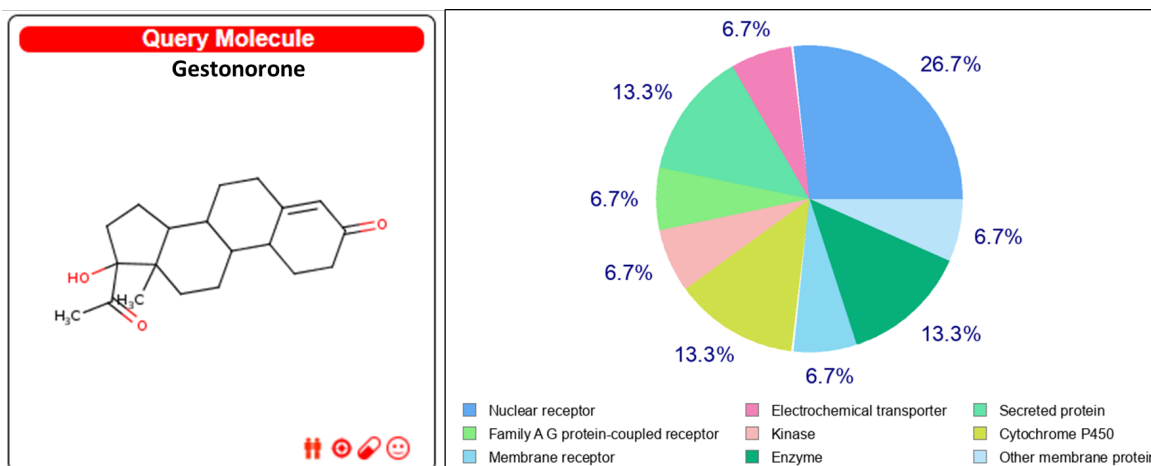
(C) Cinnamolaurine structure and Pie chart indicating Target proteins class distribution



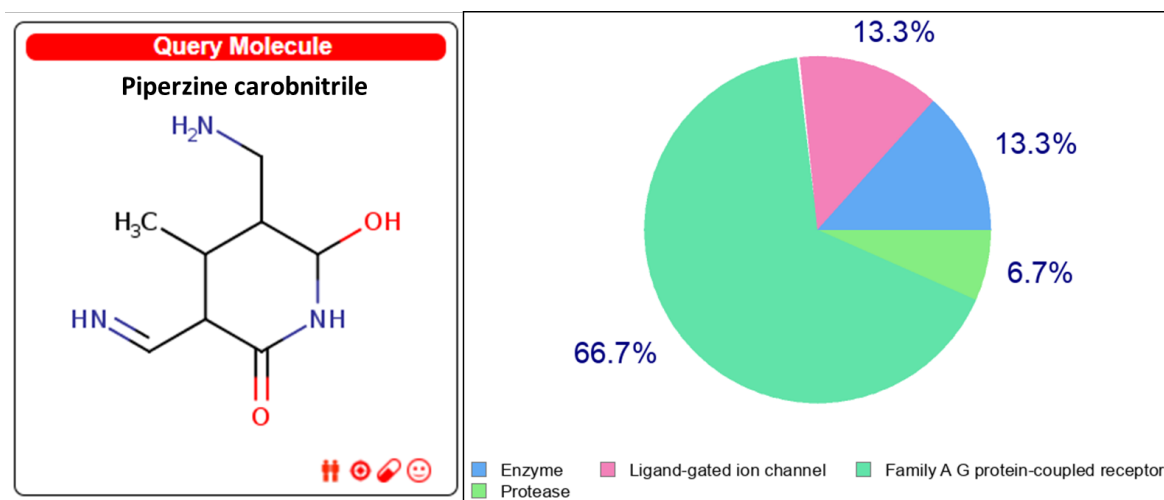
(D) Cinnamon structure and Pie chart indicating Target proteins class distribution



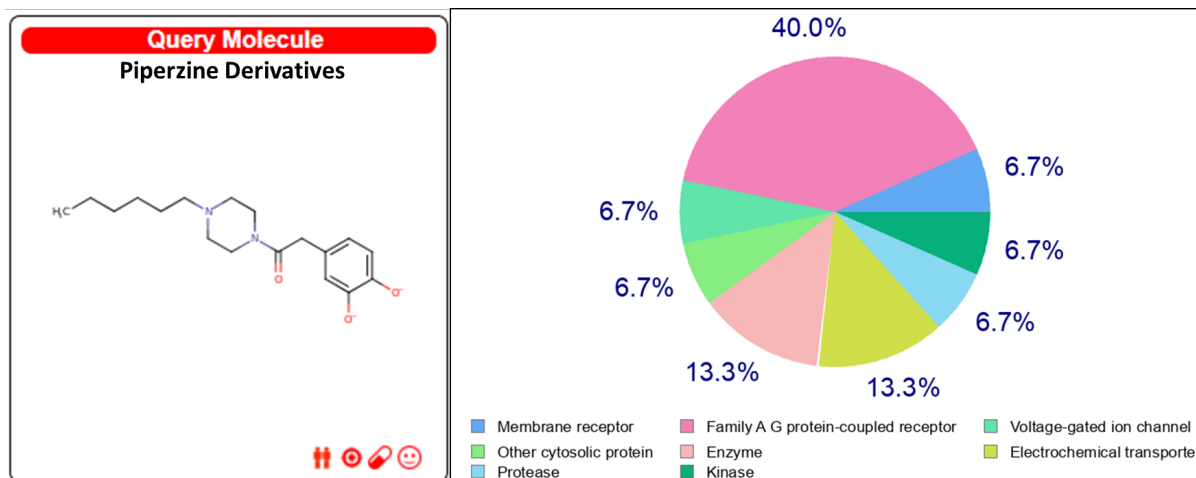
(E) Crinamine structure and Pie chart indicating Target proteins class distribution



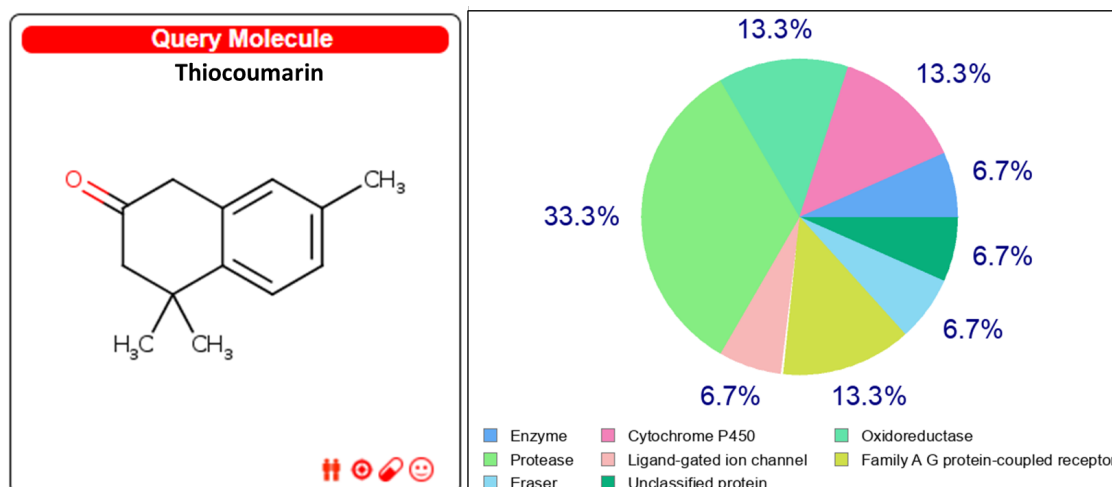
(F) Gestonorone structure and Pie chart indicating Target proteins class distribution



(G) Piperzine carbonitrile structure and Pie chart indicating Target proteins class distribution



(H) Piperzine derivative structure and Pie chart indicating Target proteins class distribution



(I) Thiocoumarin structure and Pie chart indicating Target proteins class distribution

Figure C3. 1: Structures of Phyto-compounds and respective Pie charts of molecular targets

Figure represents phyto-compound structures and respective Pie chart. Subfigure represents Pie charts of (A) Androgen, (B) Cinnamic acid, (C) Cinnamolaurine, (D) Cinnamon, (E) Crinamine, (F) Gestonorone, (G) Piperzine carbonitrile, (H) Piperzine derivative and (I) Thiocoumarin. Pie chart indicates the total proportion of protein class of that phyto-compound targets.

Besides Pie charts, software provided binding probability of each target protein for that phyto-compound along with target protein name, class and UniProt ID. Out of all the phyto-components, Androstane, Gestonorone and Cinnamolaurine showed high (≥ 0.3) binding probability. Rest of all the other components showed very less binding probability and were in the range of 0 – 0.15. All the results are mentioned in below [Table C3. 4](#) and [Table C3. 5](#).

Table C3. 4: Results of *in-silico* analysis of bioactive compound – Androstane, Cinnamic Acid, Cinnamolaurine and Cinnamon

Sr no	Compound	Target	Target Class	Probability	UniProt ID
1	Androstane	Androgen Receptor (by homology)	Nuclear receptor	0.672321428	P10275
2		Cytochrome P450 19A1	Cytochrome P450	0.593374423	P11511

Sr no	Compound	Target	Target Class	Probability	UniProt ID
3		Nuclear receptor subfamily 1 group I member 3 (by homology)	Nuclear receptor	0.348497063	Q14994
4		Carbonic anhydrase II	Lyase	0.135202128	P00918
5		Carbonic anhydrase I	Lyase	0.135202128	P00915
6		Carbonic anhydrase IV	Lyase	0.111501865	P22748
1	Cinnamic Acid	Lysosomal protective protein	Protease	0.112041901	P10619
2		Neprilysin	Protease	0.112041901	P08473
3		G-protein coupled receptor kinase 2	Kinase	0.112041901	P25098
4		Nuclear receptor subfamily 4 group A member 1	Nuclear receptor	0.112041901	P22736
5		Heat shock 70 kDa protein 1	Other cytosolic protein	0.112041901	P0DMV8
6		G protein-coupled receptor 44	Family A G protein-coupled receptor	0.112041901	Q9Y5Y4
1	Cinnamolaurine	Dopamine D2 receptor	Family A G protein-coupled receptor	0.670788316	P14416
2		Dopamine D1 receptor	Family A G protein-coupled receptor	0.642821428	P21728
3		Dopamine transporter (by homology)	Electrochemical transporter	0.632738576	Q01959
4		Serotonin 1a (5-HT1a) receptor	Family A G protein-coupled receptor	0.530019919	P08908
5		Serotonin 7 (5-HT7) receptor	Family A G protein-coupled receptor	0.237888614	P34969
6		Dopamine D3 receptor	Family A G protein-coupled receptor	0.198389229	P35462
1	Cinnamon	Glycogen synthase kinase-3 beta	Kinase	0.111501865	P49841
2		Insulin-like growth factor binding protein 3	Secreted protein	0.111501865	P17936
3		Dual-specificity tyrosine-phosphorylation regulated kinase 1A (by homology)	Kinase	0.111501865	Q13627
4		Cyclin-dependent kinase 5/CDK5 activator 1	Kinase	0.111501865	Q15078 Q00535
5		Neuronal acetylcholine receptor protein alpha-7 subunit	Ligand-gated ion channel	0.111501865	P36544

Sr no	Compound	Target	Target Class	Probability	UniProt ID
6		Dual specificity protein kinase CLK1	Kinase	0.111501865	P49759

Table C3. 5: Results of *in-silico* analysis of bioactive compound – Crinamine, Gestonorone, Thiocoumarin, Piperzine carbonitrile and it derivative

Sr no	Compound	Target	Target Class	Probability	UniProt ID
1	Crinamine	Acetylcholinesterase	Hydrolase	0.111501865	P22303
2		Delta opioid receptor	Family A G protein-coupled receptor	0.111501865	P41143
3		Transient receptor potential cation channel subfamily V member 3	Voltage-gated ion channel	0.111501865	Q8NET8
4		Glutathione reductase	Oxidoreductase	0.111501865	P00390
5		Alpha-L-fucosidase I	Enzyme	0.111501865	P04066
6		Purine nucleoside phosphorylase	Enzyme	0.111501865	P00491
1	Gestonorone	Androgen Receptor (by homology)	Nuclear receptor	0.893164792	P10275
2		Glucocorticoid receptor	Nuclear receptor	0.893164792	P04150
3		Dopamine transporter	Electrochemical transporter	0.893164792	Q01959
4		Corticosteroid binding globulin	Secreted protein	0.893164792	P08185
5		Adenosine A3 receptor	Family A G protein-coupled receptor	0.893164792	P0DMS8
6		Testis-specific androgen-binding protein	Secreted protein	0.893164792	P04278
1	Piperzine carbonitrile	Purine nucleoside phosphorylase	Enzyme	0.071787163	P00491
2		Neuronal acetylcholine receptor protein alpha-4 subunit	Ligand-gated ion channel	0.071787163	P43681
3		Beta-1 adrenergic receptor (by homology)	Family A G protein-coupled receptor	0.071787163	P08588
4		Aminopeptidase N	Protease	0.071787163	P15144

Sr no	Compound	Target	Target Class	Probability	UniProt ID
5		Beta-glucocerebrosidase	Enzyme	0	P04062
6		Alpha-1a adrenergic receptor	Family A G protein-coupled receptor	0	P35348
1	Piperzine derivatives	Sigma opioid receptor	Membrane receptor	0.159936683	Q99720
2		Mu opioid receptor	Family A G protein-coupled receptor	0.126610169	P35372
3		Delta opioid receptor	Family A G protein-coupled receptor	0.126610169	P41143
4		Kappa Opioid receptor	Family A G protein-coupled receptor	0.126610169	P41145
5		Dopamine D2 receptor	Family A G protein-coupled receptor	0.10994577	P14416
6		Dopamine D3 receptor	Family A G protein-coupled receptor	0.101613855	P35462
1	Thiocoumarin	Poly [ADP-ribose] polymerase-1	Enzyme	0.041470299	P09874
2		Cytochrome P450 26B1	Cytochrome P450	0.031226558	Q9NR63
3		Cytochrome P450 26A1	Cytochrome P450	0.031226558	O43174
4		Alcohol dehydrogenase alpha chain	Oxidoreductase	0.031226558	P07327
5		Epoxide hydrolase 1	Protease	0.031226558	P07099
6		Alcohol dehydrogenase gamma chain	Oxidoreductase	0.031226558	P00326

As Androstane, Gestonorone and Cinnamolaurine showed higher affinity compared to others, they were considered for further *in-vitro* experimentation. For the designing of gene expression assays, top three binding targets of each component were selected. These selected genes are listed in

Table C3. 6. “Dopamine D5 receptor”, top 2nd Binding Target of Cinnamolaurine, was not considered in the study due to its high structural

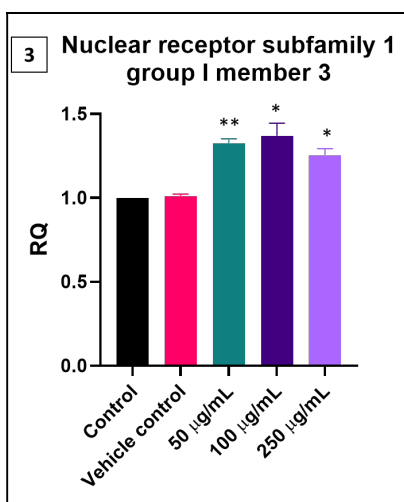
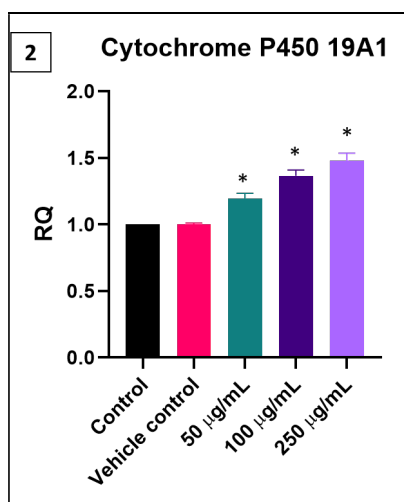
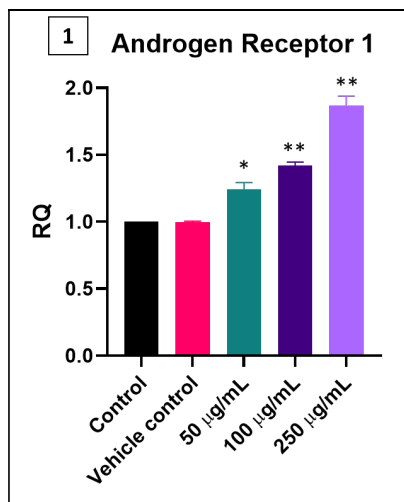
resemblance with 1st target “Dopamine D1 receptor” in terms of protein class as well as Binding Probability.

Table C3. 6: Selected Protein targets for Gene expression study

Sr no	Target	UniProt ID	Compound
1	Androgen Receptor (by homology)	P10275	Androstane, Gestonorone
2	Cytochrome P450 19A1	P11511	Androstane
3	Nuclear receptor subfamily 1 group I member 3 (by homology)	Q14994	Androstane
4	Dopamine D2 receptor	P21728	Cinnamolaurine
5	Dopamine transporter (by homology)	Q01959	Cinnamolaurine, Gestonorone
6	Glucocorticoid receptor	P04150	Gestonorone

In the gene expression study, it was observed that androgen receptor, cytochrome P450, dopamine receptor D2 and dopamine transporter were getting significantly upregulated in dose dependent manner upon LG treatment in the range of 1.39 – 2.67 times compared to control when treated with 250 µg/mL dose. At the same time, expression of GCR was significantly downregulated in dose dependent manner upon LG treatment. NR1I3 was also getting significantly upregulated upon LG treatment, but upregulation was not consistent with dose.

5.2.3 QPCR:



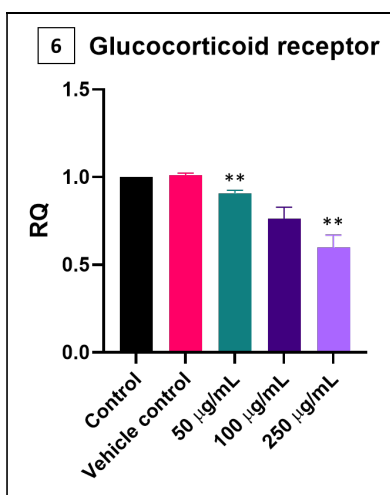
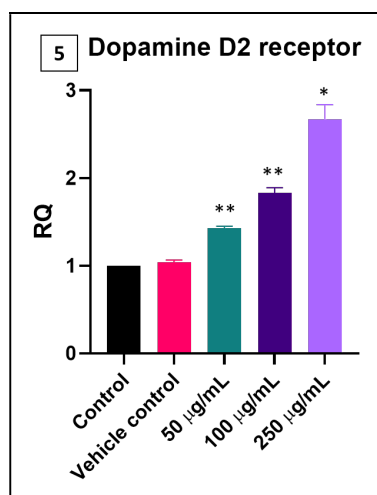
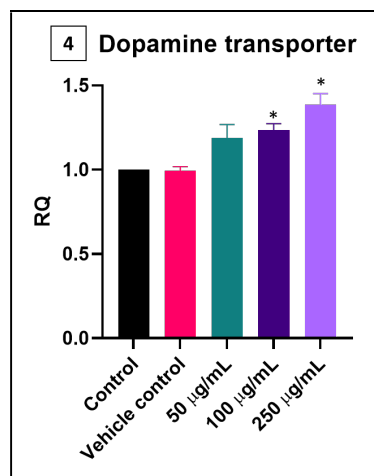


Figure C3. 2: Gene expression profile of target genes

Each graph is showing the expression profile of Target genes. It can be observed that LG upregulated dopamine receptor and

transporter, androgen receptor as well as cytochrome P450 where downregulated glucocorticoid receptor significantly. (*- $p < 0.05$; **- $p < 0.01$) All the data are presented as mean \pm S.E. and are representative of three independent experiments ($n=3$). Refer Appendix A3.1 figure of Q-PCR amplification.

Table C3. 7: Relative quantification of target genes with fold change compared to control

Target Gene	Control	Vehicle control	50 $\mu\text{g/mL}$	100 $\mu\text{g/mL}$	250 $\mu\text{g/mL}$
Dopamine D2 receptor (DRD2)	1.00 \pm 0.00	1.04 \pm 0.02	1.43 \pm 0.21	1.83 \pm 0.04	2.67 \pm 0.10
Dopamine transporter (SC6A3)	1.00 \pm 0.00	0.99 \pm 0.01	1.19 \pm 0.05	1.23 \pm 0.02	1.39 \pm 0.09
Glucocorticoid receptor (GCR)	1.00 \pm 0.00	1.01 \pm 0.01	0.91 \pm 0.10	0.76 \pm 0.04	0.60 \pm 0.14
Androgen Receptor 1 (ANDR)	1.00 \pm 0.00	1.00 \pm 0.00	1.24 \pm 0.03	1.42 \pm 0.10	1.87 \pm 0.04
Cytochrome P450 19A1 (CP19A)	1.00 \pm 0.00	1.00 \pm 0.01	1.19 \pm 0.09	1.37 \pm 0.03	1.48 \pm 0.11
Nuclear receptor subfamily 1 group I member 3 (NR1I3)	1.00 \pm 0.00	1.01 \pm 0.01	1.32 \pm 0.05	1.37 \pm 0.04	1.25 \pm 0.02

Table indicates gene fold changes of each gene upon LG treatment. Data were statically analysed using Prism software. All the data are presented as mean \pm SD and are representative of three independent experiments ($n=3$).

Table C3. 8: Significance and Standard error table of fold change value

Target Gene	Control	Vehicle control	50 $\mu\text{g/mL}$	100 $\mu\text{g/mL}$	250 $\mu\text{g/mL}$
Dopamine D2 receptor (DRD2)	0.00	0.02	0.21**	0.04**	0.10*

Target Gene	Control	Vehicle control	50 µg/mL	100 µg/mL	250 µg/mL
Dopamine transporter (SC6A3)	0.00	0.01	0.05	0.02*	0.09*
Glucocorticoid receptor (GCR)	0.00	0.01	0.11**	0.04	0.04**
Androgen Receptor 1 (ANDR)	0.00	0.00	0.03**	0.10**	0.04**
Cytochrome P450 19A1 (CP19A)	0.00	0.01	0.09*	0.03*	0.11*
Nuclear receptor subfamily 1 group I member 3 (NR1I3)	0.00	0.01	0.05**	0.04*	0.02*

Table indicates gene fold changes standard error along with significance level in form of p-value. Data were statically analysed using Prism software. *- $p < 0.05$; **- $p < 0.01$. All the data are representative of three independent experiments ($n=3$).

5.3 DISCUSSION:

Osteoporosis is the disease that results due to an imbalance of activity of osteoblasts and osteoclasts (Ge et al., 2019). Due to the serious drawbacks of currently available therapy, researchers are in the constant efforts to discover promising herbal based medicine. With the akin aim, we had conducted a study to screen all active components present in LG methanolic extract using an *in-silico* approach followed by *in-vitro* validation experiments.

Since last couple of decades, structure based drug discovery has gained a significant popularity. Advancement in information technology and development various bioinformatics software platforms have revolutionized the drug discovery approach (Kirchmair et al., 2008). *In-silico* study is the structure based drug designing and target prediction which provides insights into the interaction of a various chemical compounds with its specific target protein, yielding information about affinity and the specificity of the

interaction. The drug design and target prediction based approach aims to find out the identification of compound as well as its molecular target. For instance, where target protein or structure of target protein is unknown, ligand based target prediction approaches are employed in order to fulfil the desired information. Obtained structure or targets using such *in-silico* method are often used to design further experiments.

Molecular docking is the preferred *in-silico* technique for simulation of biomolecular interaction. Such methods hold capability to give insights into the interaction at molecular level, which provides an opportunity to study and characterize the binding and interacting site in target protein (Waghulde et al., 2018). With such bioinformatics tools, it was possible to explore the probable binding of bioactive compound of LG methanolic extract with target proteins. Androstane showed high binding probability with Androgen Receptor (by homology), Cytochrome P450 19A1, Nuclear receptor subfamily 1 group I member 3 (by homology). Out of these three, androgen receptor is a common target of Gestonorone also. *In-vitro* experiment demonstrated a significant upregulation of cytochrome P450 upon LG treatment. Cytochrome P450 is mainly responsible for the conversion of androgens to estrogen. These results clearly indicate that there is a probable role of Androstane which enhances the expression in a dose dependent manner probably leading to local estrogen level surge. These results are supported by many research groups (Simpson, 2002; Perez et al., 2006; Shaheenah et al., 2008). It was also observed that there is an upsurge in the gene expression levels of nuclear receptors like androgen receptor and nuclear receptor 113 (constitutive androstane receptor (CAR)). Studies suggest CAR and androgen receptor are closely associated with osteoblastic differentiation and bone mineralisation process (Urano et al., 2009; Roforth et al. 2012). In the present study, significant upregulation of the nuclear receptors suggests the differentiation and growth of osteoblastic cells. Therefore it also can be stated that Androstane and Gestonorone are involved in bone formation process. The study lays a strong foundation, where the similar alteration was found in *in-vivo* assessment proposing osteoprotective effect of LG (Parikh, 2009).

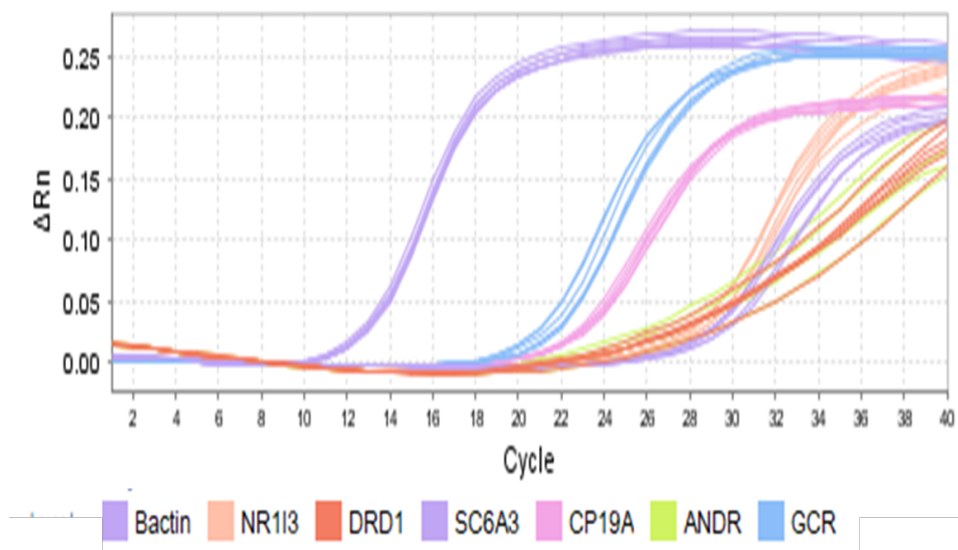
In the *in-silico* study, it was observed that Cinnamolaurine exhibited a greater probability of binding with proteins like Dopamine receptor D1R, D2R and Dopamine transporter, a common target of Gestonorone also. Dopamine which is an important neurotransmitter, exerts its effect by binding with five different types of dopamine receptors of which, receptors D1R and D2R are expressed on Osteoblasts (Cheong et al., 2018). Correlating the literature studies between dopamine and osteoblasts, dopamine has been shown to be involved in bone metabolism via playing positive role in proliferation of osteoblastic cells, bone mineralization and formation (Bliziotis et al., 2002; Lee D J et al., 2015). Elaborating *in-vitro* outcomes, dose dependent significant upregulation of dopamine receptor D2R and transporter indicates that Cinnamolaurine and Gestonorone may be involved in upregulation of these genes and hence in osteoblast proliferation. Thus, this findings elucidates the bioactive properties of Cinnamolaurine & Gestonorone found in LG extract and thus can be accounted for improving bone health.

Besides dopamine transporter and androgen receptor, Gestonorone showed a very high binding probability with Glucocorticoid receptor also. Gestonorone shows a very high binding probability with Glucocorticoid receptor which are distributed on cells of most of the tissues. It has been claimed that glucocorticoid reduces the differentiation and growth of osteoblast thus resulting in bone loss. Additionally, direct effects of glucocorticoids on osteocytes frequently lead to osteocyte death (O'Brien et al. 2004; Rauch et al., 2010; Hachemi et al. 2018). In the *in-vitro* experiment of the present study, it was observed that there is significant down-regulation of Glucocorticoid receptor in Saos-2 cell line upon LG treatment. This finding enlightens an active involvement of Gestonorone in regulating glucocorticoid receptor and hence probably playing a crucial role in suppressing bone loss activities, supporting an anti-osteoporotic property of LG. Compared to similar action(s) of other bioactive compounds, Gestonorone, supports anti-osteoporotic property of LG via bone formatting and bone loss suppression.

Cumulatively, it can be concluded that all three bioactive components play an essential role in modulating the expression of various genes. Expression

profile mapping of these genes draws a frame work of mechanistic action of LG by defining specific role of potent components in the direction of bone formation and preventing osteoporosis.

APPENDIX A3.1 FIGURE:



Appendix figure represents the amplification curve of one of the triplicate runs of the gene expression study of various receptors and enzymes which was performed post in-silico outcomes. Curve is plotted by Applied Biosystems StepOne Software v2.3. Y axis represents Fluorescence collected by the detector and X axis represents no. of cycle. Each target gene represents different samples like host, vehicle control, test 50 $\mu\text{g}/\text{mL}$, 100 $\mu\text{g}/\text{mL}$ and 250 $\mu\text{g}/\text{mL}$.